Semi-analytical computation of the acoustic response of arbitrarily shaped objects

Volker, A.W.F.; Ter Morshuizen, M.G.
TNO Institute of Applied Physics
Stieltjesweg 1 Delft
The Netherlands
T: +31 15 269 2023; +31 15 269 2030
F: +31 15 269 2111
E: volker@tpd.tno.nl; morshuizen@tpd.tno.nl

ABSTRACT

A fast, semi-analytical modeling algorithm has been developed to compute acoustic wave fields as reflected by arbitrary shaped objects for arbitrary source-receiver configurations. Examples are the computation of the target strength of submarines or mines. Other applications are the design of ultrasonic transducers with complex shapes and the analysis of configurations for non-destructive testing.
The method comprises of two steps: first, a triangular grid of the object is constructed, and second, the acoustic response is computed analytically for each grid element by using the well-known Fraunhofer approximation. Summation over all elements yields the acoustic response of the object.

INTRODUCTION

In many applications the acoustic response of arbitrarily shaped objects is studied. In situations where physical experiments are too expensive or otherwise unfeasible the answer is sought in modeling. In literature many papers have been written on the subject of modeling the acoustic wave field emitted by an insonified object. In general the presented algorithms address specific phenomena involved in the interaction between the incident wave field and the object. As a result the proposed modeling technique is only valid in a certain frequency range with respect to the dimensions of the object under study.

In literature often the dimensionless quantity "ka" (the *Helmholtz number*) is used to specify the frequency range, where k is the wavenumber (unit 1/m) and a a characteristic dimension of the object (unit m). In short, the following rather arbitrary distinction between the "high" and "low" frequency ranges can be made. If ka is less than about 10 (less than 1.5 wavelengths in a), we are in the low-frequency regime and have to use elastic vibration theory and may introduce low-frequency approximations. For ka larger than about a 100 (larger than 15 wavelengths in a), we are in the high-frequency regime and are allowed to use simple scattering principles and high-frequency approximations. In the intermediate range ($10<ka<100$), both scattering and vibration phenomena may be important to consider.

Most published methods address the low-frequency regime because they are restricted by the available computational resources. Often only results on simple shapes (spheres, plates and cylinders) are reported. Examples are finite element, boundary element and finite difference methods (FEM, BEM and FD). To obtain accurate results the volume under study (FEM) or the surface of the volume (BEM) must be densely discretised with respect to the frequency.

Another example for modeling the response of general geometries is use of the Kirchhoff approximation. The arbitrary curved scattering surface is discretised by subdividing it into a number of small flat surfaces (*facets*). For each facet the scattering contribution is calculated using the incident wavefield and the Kirchhoff approximation, assuming local plane-wave reflection on the facet. Then, the responses of all facets are added to compute the total scattered wavefield [3,4]. Note that the method is limited to scattering and more complicated elastic wave phenomena such as surface waves (Lamb, Rayleigh), vibration, wave-conversion and re-radiation are not accounted for. Multiple reflection between different surfaces must be accounted for explicitly. Facets must be smaller than the wavelength. The amount of required computational resources becomes unacceptably high for larger structures and / or higher frequencies. In this paper a semi-analytical algorithm is proposed to tackle this problem in an efficient manner.

MODELING APPROACH

Consider an arbitrary shaped object (see figure #) in a background medium. It is our objective to compute the reflected wave field due to this object for an arbitrary source-detector configuration. In principle, the reflected wave field can be computed by (ref Berkhout 1984):

$$P(\mathbf{r}_d,\mathbf{r}_s,w)=\int\int W(\mathbf{r}_d,\mathbf{r}',w)R(\mathbf{r}',\mathbf{r})W(\mathbf{r},\mathbf{r}_s,w)S(\mathbf{r}_s,w)d\mathbf{r}'d\mathbf{r}\,, \qquad (1)$$

where $S(\mathbf{r}_s,w)$ is the source wavelet at position $\mathbf{r}_s=(x_s,y_s,z_s)$, the operators $W(\mathbf{r},\mathbf{r}_s,w)$ and $W(\mathbf{r}_d,\mathbf{r}',w)$ describe wave propagation through the medium. The operator $R(\mathbf{r}',\mathbf{r})$ describes full angle dependent reflectivity in the space frequency domain. The reflected wave field is detected at $\mathbf{r}_d=(x_d,y_d,z_d)$ and denoted as $P(\mathbf{r}_d,\mathbf{r}_s,w)$.

In order to simplify our task, we will assume a locally reacting reflector, i.e., no angle dependent reflectivity. In that case equation (1) simplifies to:

$$P(\mathbf{r}_d,\mathbf{r}_s,w)=\int W(\mathbf{r}_d,\mathbf{r},w)R(\mathbf{r})W(\mathbf{r},\mathbf{r}_s,w)S(\mathbf{r}_s,w)d\mathbf{r}\,. \qquad (2)$$

Assuming a homogeneous background medium, the propagation operators can be approximated by assuming $kr>>1$, where k is the wavenumber:

$$W(\mathbf{r},\mathbf{r}_s,w)\approx\frac{jk}{2p}\frac{\cos j_s}{r_s}e^{-jkr_s}\,, \qquad (3)$$

and

$$W(\mathbf{r}_r,\mathbf{r},w)\approx\frac{jk}{2p}\frac{\cos j_r}{r_r}e^{-jkr_r}\,, \qquad (4)$$

where

$$r_s=\sqrt{(x-x_s)^2+(y-y_s)^2+(z-z_s)^2}\,, \qquad (5)$$

and

$$r_r=\sqrt{(x_r-x)^2+(y_r-y)^2+(z_r-z)^2}\,. \qquad (6)$$

The angles φ_s and φ_r are the emerge angles at the source and the reflection point at the object.

A mesh grid will be used to describe the shape of the object. Each mesh element describes a small part of the object. Each mesh element defines an arbitrary dipping plane, which closely matches the local curvature of the object. In general, a dipping plane can be describe by:

$$z=a(x-x_c)+b(y-y_c)+z_c\,. \qquad (7)$$

This plane is centered around the point (x_c,y_c,z_c). The dip of the plane is determined by the parameters *a* and *b* in the x- and y-direction respectively. Substitution of equation (7) in equation (5) and (6) yields:

$$r_s=\sqrt{(x-x_s)^2+(y-y_s)^2+(a(x-xc)+b(y-yc)+z_c-z_s)^2} \qquad (8)$$

and

$$r_r=\sqrt{(x_r-x)^2+(y_r-y)^2+(z_r-a(x-x_c)-b(y-y_c)-z_c)^2}\,. \qquad (9)$$

It is assumed that the dimensions of the mesh element are sufficiently small compared to the distance to the source and detector so the distances r_s and r_r can be linearised around the center $\mathbf{r}_c=(x_c,y_c,z_c)$. The distance of the source and receiver to the center of the mesh element is given by:

$$r_{sc}=\sqrt{(x_c-x_s)^2+(y_c-y_s)^2+(z_c-z_s)^2} \qquad (10)$$

and

$$r_{cr} = \sqrt{(x_r - x_c)^2 + (y_r - y_c)^2 + (z_r - z_c)^2}\ . \qquad (11)$$

Since the distances r_s and r_r are large with respect to the dimensions of the mesh element, we can linearise these distances around the centre of the mesh element. The Taylor expansions of source-mesh element distance and the mesh element -receiver distance are given by the following equations:

$$r_s \approx r_{sc} + \left.\frac{\partial r_s}{\partial x}\right|_{\mathbf{r}_c}(x - x_c) + \left.\frac{\partial r_s}{\partial y}\right|_{\mathbf{r}_c}(y - y_c) = r_{sc} + \frac{x_c - x_s + a(z_c - z_s)}{r_{sc}}(x - x_c) + \frac{y_c - y_s + b(z_c - z_s)}{r_{sc}}(y - y_c) \qquad (12)$$

and

$$r_r \approx r_{cr} + \left.\frac{\partial r_r}{\partial x}\right|_{\mathbf{r}_c}(x - x_c) + \left.\frac{\partial r_r}{\partial y}\right|_{\mathbf{r}_c}(y - y_c) = r_{cr} - \frac{x_r - x_c + a(z_r - z_c)}{r_{cr}}(x - x_c) - \frac{y_r - y_c + b(z_r - z_c)}{r_{cr}}(y - y_c)\cdot \qquad (13)$$

The factors a and b are related to the dip-angle of the scattering plane by the following equations:

$$a = \tan\alpha \qquad (14)$$

and

$$b = \tan\beta\ . \qquad (15)$$

We will now define the following angles:

$$\sin\theta_{sc}\cos\phi_{sc} = \frac{x_c - x_s}{r_{sc}}, \qquad (16)$$

$$\sin\theta_{sc}\sin\phi_{sc} = \frac{y_c - y_s}{r_{sc}}, \qquad (17)$$

$$\sin\theta_{cr}\cos\phi_{cr} = \frac{x_c - x_r}{r_{cr}}, \qquad (18)$$

$$\sin\theta_{cr}\sin\phi_{cr} = \frac{y_c - y_r}{r_{cr}}\ . \qquad (19)$$

Hence substitution in equations (9) and (10) yields:

$$r_s \approx r_{sc} + (\sin\theta_{sc}\cos\phi_{sc}\cos\alpha + \cos\theta_{sc}\sin\alpha)\frac{(x - x_c)}{\cos\alpha} + (\sin\theta_{sc}\sin\phi_{sc}\cos\beta + \cos\theta_{sc}\sin\beta)\frac{(y - y_c)}{\cos\beta} \qquad (20)$$

and

$$r_r \approx r_{cr} + (\sin\theta_{cr}\cos\phi_{cr}\cos\alpha + \cos\theta_{cr}\sin\alpha)\frac{(x - x_c)}{\cos\alpha} + (\sin\theta_{cr}\sin\phi_{cr}\cos\beta + \cos\theta_{cr}\sin\beta)\frac{(y - y_c)}{\cos\beta}\ . \qquad (21)$$

These approximations will be used in order to simplify the integral in equation (2):

$$P(\vec{r}_r, \vec{r}_s) = \frac{k^2}{4\pi^2}\frac{\cos\theta_{sc}}{r_{sc}}\frac{\cos\theta_{cr}}{r_{cr}}e^{-jk(r_{sc}+r_{cr})}\iint R(x,y,z)e^{-j\left(k_{x,sc}+k_{x,cr}\right)\frac{(x-x_c)}{\cos\alpha}}e^{-j\left(k_{y,sc}+k_{y,cr}\right)\frac{(y-y_c)}{\cos\beta}}dxdy, \qquad (22)$$

where $k_{x,sc} = k(\sin\theta_{sc}\cos\phi_{sc}\cos\alpha + \cos\theta_{sc}\sin\alpha)$,

$k_{y,sc} = k(\sin\theta_{sc}\sin\phi_{sc}\cos\beta + \cos\theta_{sc}\sin\beta)$,

$k_{y,cr} = k(\sin\theta_{cr}\cos\phi_{cr}\cos\alpha + \cos\theta_{cr}\sin\alpha)$

and $k_{y,cr} = k(\sin\theta_{cr}\sin\phi_{cr}\cos\beta + \cos\theta_{cr}\sin\beta)$.

Note that these approximations are only used in the phase terms. The amplitude terms require a lower degree of accuracy. In conclusion the acoustical can be obtained by a Fourier transformation of the object. This approximation is known as the Fraunhofer approximation.
The boundaries of the integration define the shape of the mesh element. In the next section, equation (22) will be evaluated for a triangular shaped mesh element.

REFLECTION RESPONSE FOR A SINGLE TRIANGLE

The triangle is a commonly used shape in the grid representation of an object. Therefore we will compute the response of a triangle analytically. In order to simplify the integral we assume that one of the corners of the triangle equals 90°. Note that this is no limitation of the method since each triangle can be decomposed in two right-angled triangles. We have to distinguish between two types of right-angled triangles, the ones with right angle on the right-hand side (Figure 1a) and the ones with the right angle on the left-hand side. The slope can either be positive or negative. This effects the integration boundaries, since the base of the triangle remains at $y = 0$. The integration boundaries of the y-coordinate have to be interchanges. Apart from an additional minus-sign, the response is the same.

The following integral has to be evaluated for a right-angled triangle (situation in Figure 1a):

$$P(\vec{r}_r,\vec{r}_s)=\frac{k^2}{4p^2}R\frac{\cos j_{sc}}{r_{sc}}\frac{\cos j_{cr}}{r_{cr}}e^{-jk(r_{sc}+r_{cr})}\int_{x_c-x_m}^{x_c+x_m}\int_{y=0}^{c(x-x_c)+cx_m}e^{-j(k_{x,sc}+k_{x,cr})\frac{(x-x_c)}{\cos a}}e^{-j(k_{y,sc}+k_{y,cr})\frac{(y-y_c)}{\cos b}}dxdy \qquad \textbf{(23)}$$

where c is the slope.

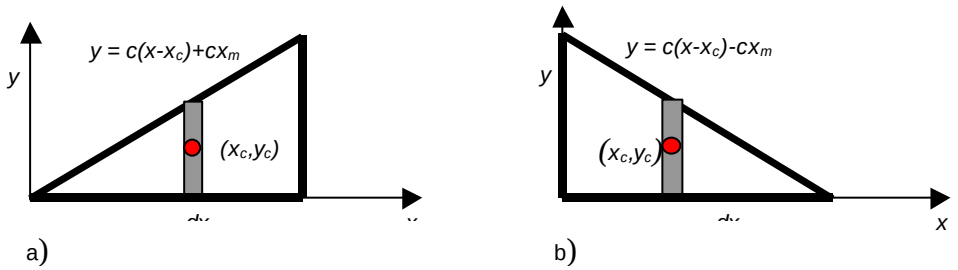

Figure 1. ***Schematic representation of integration boundary for the different types of triangles.***

For the situation Figure 1b the integral reads:

$$P(\vec{r}_r,\vec{r}_s)=\frac{k^2}{4p^2}R\frac{\cos j_{sc}}{r_{sc}}\frac{\cos j_{cr}}{r_{cr}}e^{-jk(r_{sc}+r_{cr})}\int_{x_c-x_m}^{x_c+x_m}\int_{0}^{y=c(x-x_c)-cx_m}e^{-j(k_{x,sc}+k_{x,cr})\frac{(x-x_c)}{\cos a}}e^{-j(k_{y,sc}+k_{y,cr})\frac{(y-y_c)}{\cos b}}dxdy. \qquad \textbf{(24)}$$

The solution of equation (24) will be more or less the same as of equation (23) apart from some minor details. We will only discuss the solution of the integral for equation (23). The integration over the y-coordinate is carried out first:

$$P(\vec{r}_r,\vec{r}_s)=\frac{k^2}{4p^2}R\frac{\cos j_{sc}}{r_{sc}}\frac{\cos j_{cr}}{r_{cr}}e^{-jk(r_{sc}+r_{cr})}\left(\frac{j\cos b}{k_{y,sc}+k_{y,cr}}\right)\int_{x_c-x_m}^{x_c+x_m}e^{-j\left[\frac{k_{x,sc}+k_{x,cr}}{\cos a}+c\frac{k_{y,sc}+k_{y,cr}}{\cos b}\right](x-x_c)}e^{-j(k_{y,sc}+k_{y,cr})\frac{(cx_m-y_c)}{\cos b}}-e^{-j\left(\frac{k_{x,sc}+k_{x,cr}}{\cos a}\right)(x-x_c)}e^{-j(k_{y,sc}+k_{y,cr})\frac{y_c}{\cos b}}dx. \qquad \textbf{(25)}$$

The remaining integral only depends on the x-coordinate. Integration over the x-coordinate yields the response of a single right-angled triangle:

$$P(\vec{r}_r,\vec{r}_s)=\frac{k^2}{4p^2}R\frac{\cos j_{sc}}{r_{sc}}\frac{\cos j_{cr}}{r_{cr}}e^{-jk(r_{sc}+r_{cr})}\left(\frac{j\cos b}{k_{y,sc}+k_{y,cr}}\right)\left\{\frac{2\sin\left(\left[\frac{k_{x,sc}+k_{x,cr}}{\cos a}+c\frac{k_{y,sc}+k_{y,cr}}{\cos b}\right]x_m\right)}{\frac{k_{x,sc}+k_{x,cr}}{\cos a}+c\frac{k_{y,sc}+k_{y,cr}}{\cos b}}e^{-j\left(\frac{k_{y,sc}+k_{y,cr}}{\cos b}\right)(cx_m-y_c)}-\frac{2\sin\left(\frac{k_{x,sc}+k_{x,cr}}{\cos a}x_m\right)}{\frac{k_{x,sc}+k_{x,cr}}{\cos a}}e^{j\frac{(k_{y,sc}+k_{y,cr})}{\cos b}y_c}\right\}. \qquad \textbf{(26)}$$

This equation can be rewritten as:

$$P(\vec{r}_r,\vec{r}_s)=\frac{k^2}{4p^2}R\frac{\cos j_{sc}}{r_{sc}}\frac{\cos j_{cr}}{r_{cr}}e^{-jk(r_{sc}+r_{cr})}\left(\frac{j}{k_2}\right)\left\{\frac{2\sin\left([k_1+ck_2]x_m\right)}{k_1+ck_2}e^{-jk_2(cx_m-y_c)}-\frac{2\sin\left(k_1x_m\right)}{k_1}e^{jk_2y_c}\right\}, \qquad \textbf{(27)}$$

where

$$k_1=\frac{k_{x,sc}+k_{x,cr}}{\cos a}, \qquad \textbf{(28)}$$

and

$$k_2=\frac{k_{y,sc}+k_{y,cr}}{\cos b}. \qquad \textbf{(29)}$$

Equation (27) has a number of singular points. The limit with respect to these points should have a finite value in order to be a physically acceptable solution. It can be shown that this is indeed the case. In the derivation of the response of a triangle we have assumed that the triangle has the same orientation as in Figure 1. In general the triangles will have an arbitrary orientation. With a simple rotation each triangle can be transformed according to Figure 1. This is illustrated in Figure 2. After the rotation the triangle is split in two right-angled triangles to facilitate a simple computation of its acoustic response. Note that of course the source and receiver coordinates are also rotated in order to keep the configuration consistent.

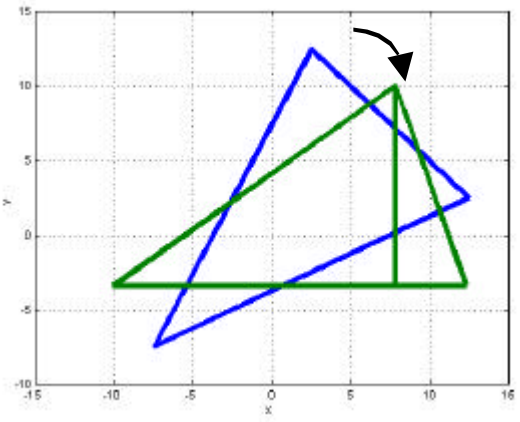

Figure 2. ***Rotation of triangle in order to compute its acoustic response. The original triangle is rotated in such a way that one of the sides is along the horizontal direction.***

GRID SIZE

In order to obtain reasonable accuracy of the results the grid-element size should be determined carefully. One does not want to use a very fine grid because of the computational cost. On the other hand a too coarse grid yields inaccurate results.

There are two criteria for selecting a proper grid spacing. Obviously the grid should be able to follow the curvature of the object. The difference between the real shape and the grid should be small compared to the acoustic wavelength. A commonly applied criterion is that the maximum error should be in the order of a tenth of the wavelength.

Furthermore the grid spacing should be small enough to ensure that the applied linearisation is accurate. For this case the following criterion applies:

$$\Delta x<\sqrt{rl}=\sqrt{\frac{rc_p}{f}}, \qquad \textbf{(30)}$$

where Äx equals the typical grid size, *r* is the distance to the reflecting object and ë is the wavelength of the signal. Note that this is not a very strict criterion for example using *r* = 100 m and ë = 0.3 m (*f* = 5 kHz, C_p = 1500 m/s), the grid spacing may still be as large as 5.5 m! In practice, this means that the curvature of the object determines the dimensions of the grid.

EXAMPLES: ACOUSTICAL RESPONSE OF A CYLINDER

To evaluate the algorithm the acoustic response of a cylinder will be compute for a rectangular and a triangular mesh. An analytical expression for the target strength of a cylinder exists. This will be used to verify the results.

The far field target strength of a cylinder [2] is given by:

$$TS = \frac{aL^2}{2l}\left(\frac{\sin(kL\sin q)}{kL\sin q}\cos q\right)^2. \qquad (31)$$

The cylinder has a length of 40 m and a diameter of 8 m. The source and receiver are 10 km away from the cylinder. This is sufficient to obtain the far field response.

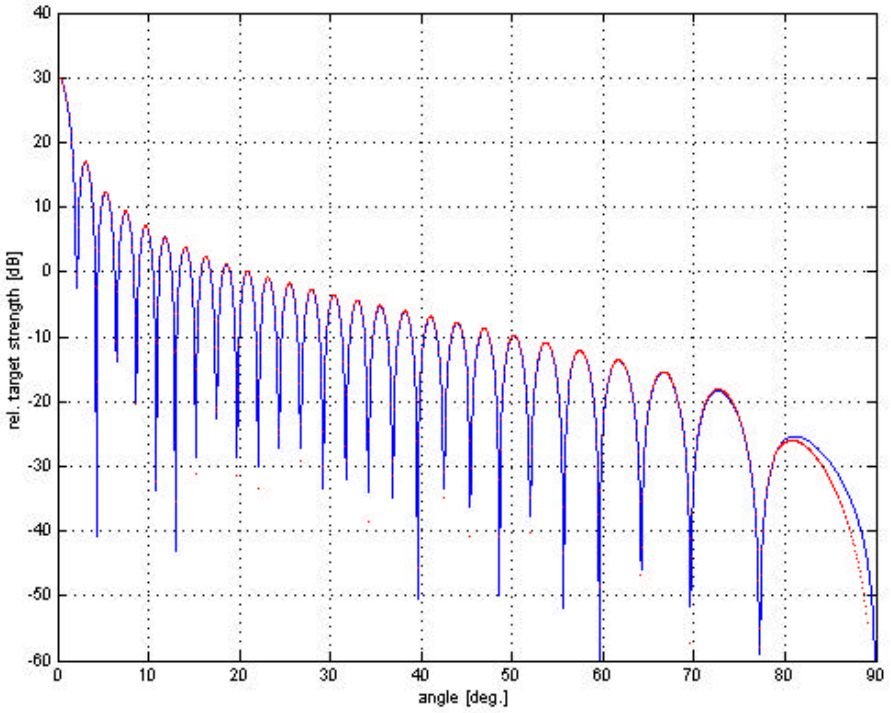

Figure 3. ***Simulated and computed target strength, using equation (31). The simulation results match very well with the analytical expression.***

CONCLUSIONS

Many methods for accurate modeling of the acoustic response (reflection and scattering) of arbitrary shaped objects are limited by available computational resources. The semi-analytical approach presented in this paper tackles this problem. First the surface of the object under study is divided into grid of triangles. Then the response of each triangle is calculated by a Fraunhofer approximation and finally all contributions of the triangles are added resulting in the acoustic response of the object.

As shown, the size of the elements is not restricted by the wavelength but rather by the curvatures of the object. Practically, this means that flat portions of the object can be meshed by several triangles, while the number of triangles is increased at strongly curved parts. As a result the total amount of triangles can be limited, reducing the required amount of resources. This makes the proposed method accurate, fast and flexible.

REFERENCES

[1] Berkhout, 1985, Seismic migration; A. Theoretical aspects, Elsevier science publishers, Amsterdam.

[2] R.J. Urick, 1983, Principles of underwater sound 3rd edition Peninsula Publishing, Los Altos, California.

[3] George O; Bahl, R., 1995, *Simulation of backscattering of high frequency sound from complex object and sand sea-bottom*, IEEE-Journal-of-Oceanic Engineering (USA), vol. 20, no.2, pp 119-130, April 1995.

[4] Brill, D; Gaunnard, G.C., 1990, *High frequency monostatic echoes from finite-length cylinders*, First French Conference on Acoustics, Lyon, France, 10-13 April 1990. In: Colloque-de-dePhysique (France), no.C-2, pt.1, pp383-386, Feb. 1990. RN ISSN: 0449-1947.